Published in final edited form as:
Lancet. 2010 August 7; 376(9739): 440–448. doi:10.1016/S0140-6736(10)60668-X.

Regeneration of the articular surface of the rabbit synovial joint by cell homing: a proof of concept study

Chang H Lee, PhD, **James L Cook, DVM**, **Avital Mendelson, MS**, **Eduardo K Moioli, PhD**, **Hai Yao, PhD**, and **Prof. Jeremy J Mao, PhD**
Columbia University Medical Center, Tissue Engineering and Regenerative Medicine Laboratory, New York, NY, USA (C H Lee PhD, A Mendelson MS, E K Moioli PhD, Prof J J Mao PhD); University of Missouri, College of Veterinary Medicine and School of Medicine, Comparative Orthopaedic Laboratory, Columbia, MO, USA (J L Cook DVM); and Clemson University and Medical University of South Carolina, Department of Bioengineering, Charleston, SC, USA (H Yao PhD)

Summary

Background—A common approach for tissue regeneration is cell delivery, for example by direct transplantation of stem or progenitor cells. An alternative, by recruitment of endogenous cells, needs experimental evidence. We tested the hypothesis that the articular surface of the synovial joint can regenerate with a biological cue spatially embedded in an anatomically correct bioscaffold.

Methods—In this proof of concept study, the surface morphology of a rabbit proximal humeral joint was captured with laser scanning and reconstructed by computer-aided design. We fabricated an anatomically correct bioscaffold using a composite of poly-ε-caprolactone and hydroxyapatite. The entire articular surface of unilateral proximal humeral condyles of skeletally mature rabbits was surgically excised and replaced with bioscaffolds spatially infused with transforming growth factor β3 (TGFβ3)-adsorbed or TGFβ3-free collagen hydrogel. Locomotion and weightbearing were assessed 1–2, 3–4, and 5–8 weeks after surgery. At 4 months, regenerated cartilage samples were retrieved from in vivo and assessed for surface fissure, thickness, density, chondrocyte numbers, collagen type II and aggrecan, and mechanical properties.

Findings—Ten rabbits received TGFβ3-infused bioscaffolds, ten received TGFβ3-free bioscaffolds, and three rabbits underwent humeral-head excision without bioscaffold replacement. All animals in the TGFβ3-delivery group fully resumed weightbearing and locomotion 3–4 weeks after surgery, more consistently than those in the TGFβ3-free group. Defect-only rabbits limped at

Correspondence to: Prof Jeremy J Mao, Columbia University Medical Center, 630 W 168 St – PH7E, New York, NY 10032, USA, jmao@columbia.edu.

Contributors
CHL was responsible for the primary technical undertaking and technical design, did the experiments, and drafted the report. JLC participated in the overall design, especially the surgical design and animal model, and did all animal surgeries. AM did the in-vitro cell homing experiment. EKM contributed to the technical design of the biomaterials and participated in animal surgery. HY did μCT analysis. JJM conceived and designed the experiments, and oversaw the collection of results, data interpretation and finalised the report.

Conflicts of interest
We declare that we have no conflicts of interest.

all times. 4 months after surgery, TGFβ3-infused bioscaffolds were fully covered with hyaline cartilage in the articular surface. TGFβ3-free bioscaffolds had only isolated cartilage formation, and no cartilage formation occurred in defect-only rabbits. TGFβ3 delivery yielded uniformly distributed chondrocytes in a matrix with collagen type II and aggrecan and had significantly greater thickness ($p=0{\cdot}044$) and density ($p<0{\cdot}0001$) than did cartilage formed without TGFβ3. Compressive and shear properties of TGFβ3-mediated articular cartilage did not differ from those of native articular cartilage, and were significantly greater than those of cartilage formed without TGFβ3. Regenerated cartilage was avascular and integrated with regenerated subchondral bone that had well defined blood vessels. TGFβ3 delivery recruited roughly 130% more cells in the regenerated articular cartilage than did spontaneous cell migration without TGFβ3.

Interpretation—Our findings suggest that the entire articular surface of the synovial joint can regenerate without cell transplantation. Regeneration of complex tissues is probable by homing of endogenous cells, as exemplified by stratified a vascular cartilage and vascularised bone. Whether cell homing acts as an adjunctive or alternative approach of cell delivery for regeneration of tissues with different organisational complexity warrants further investigation.

Funding—New York State Stem Cell Science; US National Institutes of Health.

Introduction

Tissue or organ defect is the final outcome of all incurable diseases. An organ consists of dissimilar tissues, and every tissue is formed of one or more cell types. For decades, cell-based approaches have been used to replace diseased cells and to heal tissue defects.1–5 Cell delivery has, however, encountered crucial barriers in therapeutic translation, including immune rejection, pathogen transmission, potential tumorigenesis, issues with packaging, storage, and shipping, and difficulties in clinical adoption and regulatory approval.6–8 Tissue regeneration by recruitment of the host's endogenous cells, including stem or progenitor cells, is an emerging idea. However, tissue regeneration by cell homing, especially without cell transplantation, remains a provocative approach in need of experimental testing.9–12

The synovial joint consists of multiple tissues including articular cartilage, subchondral bone, haemtopoietic marrow, and synovium. Osteoarthritis manifests as structural breakdown of cartilage and bone, and is a leading chronic disability worldwide, affecting about 80 million individuals in the USA alone.13,14 At present, arthritic joints are replaced by total joint arthroplasty using metallic and synthetic materials. Existing joint prostheses fail mainly because of aseptic loosening or infection induced by wear debris.13–15 Given an average lifespan of 10–15 years, metal prosthesis is problematic in the substantial and increasing population of arthritis patients who are aged 65 years or younger.13–15 Furthermore, metal prostheses do not remodel with host bone, leading to aseptic loosening, an issue that can only be solved by biological regeneration. Similar to regeneration of other tissues, cartilage regeneration is replete with examples of cell delivery.16–19 The predominant model of cartilage regeneration is focal lesions.20,21 However, focal lesions deteriorate, with or without existing interventions, into severe arthritis that ultimately warrants total joint arthroplasty.15,22,23 Commercial approaches for the treatment of focal lesions in patients are only partly successful and are associated with persistent drawbacks

such as suboptimum integration, loss of chondrocyte phenotype, and guarded functional outcome.22–24 We tested the hypothesis that the entire articular surface of the synovial joint can regenerate with a bioactive cue spatially embedded in an anatomically correct bioscaffold.

Methods

Design and fabrication of the bioscaffold

Surface morphology of the cadaver humeral head of the forelimb joint from a 6-month-old rabbit (matching those used for in-vivo experiments) was captured with multislice laser scanning at 12·7 μm resolution (Berding, Loveland, OH, USA; figure 1A), and reconstructed in three dimensions by computer-aided design (figure 1E). An anatomically correct bioscaffold measuring 12·42×10·11×16·88 mm^3 (length×width×height) was designed to replace the condylar head, with an intramedullary stem for surgical fixation (figure 1B). This overall dimension is far greater than the capacity for diffusion exchange of regenerating tissues, which is about 200 μm.25 Accordingly, we designed three-dimensional interconnecting microchannels (200–400 μm diameter) as conduits to promote tissue regeneration (figure 1C, D). We fabricated the bioscaffold using three-dimensional layer-by-layer bioprinting; 20 wt% hydroxyapatite (HA) powder (Sigma, St Louis, MO, USA) into 80 wt% poly-ε-caprolactone (PCL; molecular weight roughly 65 000, Sigma) slurry at 120°C (Bioplotter, EnvisionTec, Gladbeck, Germany). We selected PCL-HA in accordance with our previous finding of cell adhesion and osteochondral histogenesis using the same materials.26 Figure 1C shows the superior portion of the bioscaffold, with the top 500 μm designed for regeneration of cartilage, similar to the thickness of the native rabbit humeral articular cartilage. Figure 1D shows the inferior portion, which was designed for regeneration of bone, with the intramedullary stem omitted for demonstration. Interlaid strands and interconnecting microchannels had diameters of 400 μm in the cartilage portion (figure 1C), and 200 μm in the bone portion (figure 1D).

TGFβ3 infusion

Transforming growth factor β3 (TGFβ3) at a dose of 10 ng/mL (Cell Biosciences, Palo Alto, CA, USA) was adsorbed in 5 mg/mL neutralised collagen type I (Cultrex, R&D, Minneapolis, MN, USA). We selected this dose of TGFβ3 to stimulate chondrogenic differentiation.26,27 TGFβ3-adsorbed or TGFβ3-free collagen solution was infused into the microchannels of the bioscaffold to a depth of roughly 500 μm, and cross-linked for 1 h at 37°C without additional cross-linker. Our rationale for 400-μm diameter microchannels in the cartilage portion of the scaffold was to provide space for matrix synthesis and anchorage for TGFβ3-loaded or TGFβ3-free collagen gels.

Surgical joint replacement

We received Institutional Animal Care and Use Committee approval to use skeletally mature New Zealand white rabbits (aged 6 months, weighing 3·5–4·0 kg; Harlan, Indianapolis, IN, USA). Skeletal maturity was defined by age (5–6 months) and bodyweight (3·5–4·0 kg), following the established criteria for cartilage regeneration.15 The rabbits were anaesthetised with ketamine (35 mg/mL) and xylazine (5 mg/mL), and maintained with 1–

5% isoflurane. With a craniolateral approach, the acromial head of the deltoid muscle was tenotomised at its origin and retracted distally. The infraspinatus muscle was tenotomised at its insertion and retracted caudally. The lateral joint capsule was incised from cranial to caudal to expose the humeral head by internal rotation and complete lateral luxation. An osteotome and mallet were used to excise the humeral head at its metaphysis junction, while preserving the greater and lesser tubercles and all soft tissue attachments (figure 1F) to simulate unipolar joint arthroplasty. A 3·2 mm drill bit on a hand chuck created an intramedullary tunnel for stem insertion (figure 1G). After humeral-head excision, the anatomically correct bioscaffold (figure 1H) was implanted by press-fitting (figure 1I). The joint capsule was closed with a mattress suture, followed by reattachment of the infraspinatus and deltoid tendons. The subcutis was apposed with 4-0 polydioxanone suture, followed by skin closure. Locomotion and weightbearing were assessed at 1–2, 3–4, 5–8 weeks postsurgery.

Histology and histomorphometric analysis

4 months after implantation, articular cartilage samples were stained with India ink and imaged with a high-resolution camera to reveal surface fissures and defects. Harvested tissue and scaffold samples were embedded in poly(methyl methacrylate) and cut into 5-μm sections (HSRL, Jackson, VA, USA). Using a random number table, we selected sections to be separately stained with safranin O, von Kossa, and haematoxylin and eosin. Cartilage thickness was measured as the linear distance from articular surface to subchondral bone at ten equally spaced locations across the entire cartilage. The areal matrix density was measured as the intensity of safranin O staining across the entire cartilage with the same microscope contrast and brightness. We counted the numbers of cells in regenerated cartilage on ten randomly selected microscopic sections per sample in each of the groups. The number and diameter of blood vessels with erythrocytes and lined by endothelial cells in regenerated subchondral bone were quantified by image analysis. All measurements were done separately by two calibrated and masked examiners. The glenoid fossae, which are the opposing articular surfaces, were harvested and fixed in 4% formaldehyde. After paraffin embedding, we cut 5-3m serial sections in the medial, central, and lateral planes (webappendix p 4).

Immunofluorescence of collagen type II and aggrecan

4 months after in-vivo implantation, we immunoblotted collagen type II and aggrecan in the cartilage matrix. Tissue samples were washed with 0·1% Triton X and incubated with monoclonal antibodies for collagen type II (1:100; CP18, Calbiochem, Gibbstown, NJ, USA) or aggrecan (1:100; ab3773, Abcam, Cambridge, MA, USA) for 1·5 h at room temperature. Before application of aggrecan antibody, samples were treated with chondroitinase ABC, keratanase, and keratanase II for 1 h. After 1-h incubation with secondary antibodies of Alexa Fluor 680 (Invitrogen, Carlsbad, CA, USA) and IRDye 800CW (LI-COR, Lincoln, NE, USA), we semiquantified samples using infrared imaging with 700-nm excitation and 800-nm emission wavelengths (Odyssey, LI-COR). The integrated intensity of fluorescence normalised to each immunoreactive area was calculated as relative immunoreactivity.

Mechanical properties of regenerated cartilage

We did compressive and shear tests using an ElectroForce BioDynamic Tester (Bose, Eden Prairie, MN, USA). Cylindrical osteochondral plugs (5·05 [SD 0·51]×5·21 [0·31] mm^2) were punched from native, TGFβ3-regenerated, and TGFβ3-free cartilage samples 4 months after in-vivo implantation. Compressive testing was done under 10% cyclic strain at 2 Hz, and shear testing with 3% sinusoidal strain under 10% compressive strain at 2 Hz.28 We characterised dynamic compressive properties as complex compressive modulus E*, storage modulus E′, and loss modulus E″, and dynamic shear properties as the complex shear modulus G*, shear storage modulus G′, and shear loss modulus G″.

Statistical analysis

All statistical analyses were done with SPSS (version 16) and PASS 2005. Power analyses were performed with a significance level of 0·05, effect size of 1·50, and power of 0·8. Effect size and power calculations were based on our pilot experiments and previous work. 26 For normal distribution, quantitative data for control and treated groups were subjected to one-way ANOVA and post-hoc least significant difference tests. For skewed data, we used non-parametric Kruskal-Wallis tests.

Role of the funding source

The funding source was not involved in the design, data collection, data analysis, data interpretation, or writing of the report. The corresponding author had full access to all data in the study and had final responsibility for the decision to submit for publication.

Results

Ten rabbits received anatomically correct bioscaffolds infused with TGFβ3-adsorbed collagen gel, and ten received bioscaffolds infused with TGFβ3-free gel. Three animals underwent condyle excision without bioscaffold replacement. Within the first 1–2 weeks after joint replacement, the representative TGFβ3-infused rabbit limped with little use of the operated right forelimb (webvideo 1). By 3–4 weeks postsurgery, the same rabbit underwent locomotion and weightbearing with all limbs including the operated one (webvideo 2). By 5–8 weeks postsurgery, the same rabbit moved (webvideo 3) almost as unoperated, age-matched rabbits. These webvideos are representative of many video-recorded animals.

4 months after humeral-head excision without bioscaffold implantation, there was little regeneration in the defect, showing synovial cavity with residual scarring fibrous tissue covering immature, woven bone and marrow (figure 1J). Safranin O staining revealed isolated chondrocyte-like cells in the defect's fibrous layer (figure 1K), but little cartilage formation. Functionally, defect-only rabbits with condyle excision limped at all times, suggesting that condylar-head ablation is a critical-size defect for both cartilage and bone. By contrast, cartilage and bonere generation occurred in bioengineered synovial joint replacements. In reference to an unimplanted bioscaffold sample (figure 2A), the TGFβ3-infused bioscaffold had full tissue coverage (figure 2C), whereas the TGFβ3-free bioscaffold had only isolated tissue formation (figure 2B). The native articular surface is shown for comparison (figure 2D).

India ink, a dye that reveals surface fissures and defects, marked the border of microchannel openings of the unimplanted bioscaffold (figure 2A), but did not stain either TGFβ3-regenerated cartilage (figure 2C) or native articular cartilage (figure 2D). By contrast, India ink stained the border of isolated cartilage tissue of the TGFβ3-free sample (figure 2B). TGFβ3 delivery recruited roughly 130% more cells in the regenerated articular cartilage than did spontaneous cell migration without TGFβ3 (figure 2E; n=8; p<0·0001), suggesting that TGFβ3 is a chemotactic cue for cell homing. Microscopically, chondrocytes in the TGFβ3-free sample clustered and synthesised matrix with positive but moderate safranin O staining (figure 2F, I).By contrast, TGFβ3 delivery yielded evenly distributed chondrocytes and intense safranin O staining for both pericellular and interterritorial matrices (figure 2G, J).

Regenerated articular cartilage in the TGFβ3-infused group extended above the bioscaffold's superior surface (figure 2C, G), suggesting that cartilage, instead of the bioscaffold, was articulating with the opposing native cartilage (glenoid) surface. Quantitatively, samples from the TGFβ3-infused group had significantly greater matrix density (figure 2H; p<0·0001) and articular cartilage thickness (figure 2K; p=0·044) than did samples from the TGFβ3-free group (n=8 per group for both comparisons). In either regenerated or native articular cartilage, fast green counterstaining was absent, suggesting paucity of fibrous tissue, by comparison with the presence of fibrous tissue or fibrocartilage in defect-only samples (figure 1J, K). Regenerated articular cartilage was derived entirely from host endogenous cells.

Immunostaining showed no autofluorescence of unimplanted bioscaffold (figure 3A–D). Collagen type II and aggrecan, two major macromolecules of articular cartilage, were present in the native cartilage sample (figure 3E–H). By contrast with uneven and isolated areas of collagen type II and aggrecan in TGFβ3-free samples (figure 3I–L), TGFβ3-regenerated samples had consistent and continuous distribution of both collagen type II and aggrecan in the articular surface and sagittal plane (figure 3M–P). Semiquantitatively, TGFβ3 delivery yielded greater collagen type II and aggrecan immunoreactivity than was seen either in the TGFβ3-free or native group (figure 3Q, R; n=10 per group), probably because of active remodelling. The glenoid fossae showed qualitatively little sign of cartilage injury or osteoarthritis in photographs and microscopic images in the medial, central, and lateral planes of TGFβ3-delivered or TGFβ3-free samples, by comparison with the native glenoid fossa (webappendix p 4).

A radiolucent region was present in the joint cavity after excision of the articular surface and subsequent implantation of the radiolucent bioscaffold (figure 4A). A convex, radio-opaque structure was present in the joint cavity of the same rabbit 8 weeks (figure 4B) and 16 weeks (figure 4C) after surgery, suggesting the formation of a mineralised condyle-like structure. The regenerated articular cartilage extended to subchondral bone (figure 4D, E). Von Kossa staining showed mineral deposition within the bioscaffold's interconnecting microchannels (figure 4F), extending from articular cartilage inferiorly along the microchannel wall (figure 4F, G). Trabecular structures were populated by columnar osteoblast-like cells (figure 4H). The regenerated subchondral bone integrated to native bone (figure 4I).

Vasculature was present in regenerated bone (figure 4J, K), but absent in regenerated articular cartilage. TGFβ3 delivery did not increase either blood vessel number (9·2 [SD 3·4] per mm^2) or vessel diameter (72·9 [46·7] μm) compared with the TGFβ3-free group (10·4 [4·5] per mm^2, 67·1 [28·4] μm; n=8; p=0·284 for vessel number; p=0·158 for vessel diameter), leading to a speculation that angiogenesis and osteogenesis can be further improved. Importantly, all blood vessels were host-derived. Whole bone and scaffold μCT images showed thorough host tissue in growth in microchannels in both TGFβ3-free and TGFβ3-infused samples (webappendix p 5).

4 months after implantation, |E*|, E′, and E″ of TGFβ3-infused articular cartilage samples did not differ from those of native articular cartilage, but were significantly higher than those of TGFβ3-free samples (figure 5; n=5 for all groups). Similarly, |G*|, G′ and G″ were significantly higher in TGFβ3-regenerated samples than in TGFβ3-free samples. |G*| and G′ did not differ between native and TGFβ3-regenerated cartilage samples, but G″ was significantly higher in native cartilage than in TGFβ3-regenerated and TGFβ3-free samples. In general, the dynamic viscoelastic moduli of the TGFβ3-infused articular cartilage were similar to those of the native articular cartilage samples.28

Discussion

Our results show that the entire articular surface of a synovial joint can be regenerated by homing of endogenous cells. Webvideos of locomotion and weightbearing of joint-replaced animals are substantiated by regeneration of avascular articular cartilage and vascularised subchondral bone, two dissimilar tissues that function in unison. We used a rabbit model, despite the opinion that focal lesions of rabbit cartilage have spontaneous healing capacity.29 However, spontaneous healing in animals the size of rabbits or smaller, if present, seems to apply only to focal defects. Notably, the present model of total condyle ablation did not spontaneously regenerate and remained a critical-size defect up to 4 months after condyle excision. With TGFβ3 delivery, however, cartilage regenerated over the bioscaffold's superior surface, and allowed functional recovery of weightbearing and locomotion. Regenerated cartilage is probably hyaline, in view of the presence of collagen type II and aggrecan and the absence of fast green staining; by contrast, fibrocartilaginous articulations such as the temporomandibular joint show strong fast green counterstaining in the superior portion of fibrocartilage.30 The probability of hyaline cartilage regeneration is further substantiated by the similar mechanical properties of TGFβ3-regenerated cartilage to those of native articular (hyaline) cartilage. In general, the compressive modulus of hyaline cartilage is about four to eight times greater than that of fibrocartilage.31

Cell homing underlies the regeneration of articular cartilage in vivo. The process of cell homing has been used to describe the extravasation of circulating cells.9,10 Here, we broadly define cell homing as the recruitment of endogenous cells to an anatomic compartment. Despite TGFβ3's broad effects on cell adhesion and differentiation, it is rarely regarded as a cell homing molecule.30,32,33 We have shown that TGFβ3 infusion recruits about 130% more cells than in the absence of TGFβ3. Formation of cartilage in the absence of TGFβ3 is likely due to spontaneous cell migration in the joint environment, similar to sparse chondrocytes in defect-only samples; however, cartilage formed in this way has low

concentrations of aggrecan and collagen type II, and poor mechanical properties. An approach similar to ours, without growth factor delivery, yielded fibrous tissue or fibrocartilage scarring and poor functional recovery,34 providing partial confirmation of our TGFβ3-free group and again underscoring the potency of bioactive cues in cartilage regeneration. The porous surface at the proximal end of our bioscaffold in the synovial cavity provided access for synovium stem or progenitor cells, which are a probable source of articular chondrocytes,35,36 just as the porous distal end provided access for bone marrow stem or progenitor cells.

We speculate that some of the endogenous cells are derived from stem or progenitor cells of synovium, bone marrow, adipose (fat pad adjacent to synovial membrane and bone marrow), and perhaps vasculature. Although subsequent studies are needed to elucidate the precise sources of endogenous cells that home to regenerate articular cartilage and subchondral bone, we have made the following initial attempts (webappendix p 6). Cells were separately isolated from regenerated articular cartilage and subchondral bone. Cells from regenerated cartilage were spherical, but assumed spindle shape after 7-day culture, whereas cells from regenerated bone maintained their initial spindle shape. Activin A, a marker preferentially expressed by bone marrow cells,37 showed little expression in cells from regenerated cartilage, but was robustly expressed in cells from regenerated bone (webappendix p 6). Furthermore TGFβ3 recruited a remarkable number of mesenchymal stem or progenitor cells and synovium stem or progenitor cells in vitro by comparison with spontaneous cell migration (webappendix p 7). We suspect that cells from several sources were recruited by TGFβ3 in the microchannels of the bioscaffold and interacted in regeneration. Delineation of endogenous cell sources will contribute to strategies that recruit specific cell populations for regeneration of complex tissues.

We have unravelled several crucial roadblocks in regenerative medicine including cell homing, angiogenesis, scale up, and tissue biophysical properties. Viscoelastic properties of TGFβ3-mediated articular cartilage are not only in the same range as those of native articular cartilage, but are also superior to those of TGFβ3-free samples, suggesting that regenerated articular cartilage has sufficient mechanical stiffness. This finding is confirmed by weightbearing and locomotion (webvideos 1–3), as well as microscopic data for articular cartilage regeneration. The biocompatible PCL-HA used to create the bioscaffold possesses sufficient mechanical stiffness for initial weightbearing. PCL can be biodegraded by hydrolysis of its ester linkages, and can be further modified, if warranted, with ring-opening polymerisation and other approaches.38

The regeneration of the entire articular surface of a synovial joint has succeeded probably because of modularisation of a large tissue scaffold with repeating and interconnecting microchannels serving as conduits for cell homing, diffusion, histogenesis, and angiogenesis. Irrespective of scaffold size, each module contains microchannel or microstrand units in the range of 200–400 μm, which seems to be a crucial threshold for survival of regenerating tissues.25 The present translational strategy provides a feasible approach for regeneration of dissimilar tissues such as avascular cartilage and vascularised bone, which constitute the entire articular surface of a synovial joint. An important extension of our work is replacement of arthritic synovial joints in preclinical models and in arthritis

patients who need total joint arthroplasty. Since cartilage, a tissue that is recalcitrant to regeneration, is regenerated by endogenous cells that are recruited from the host, there is reason to believe that other tissues could also regenerate without cell transplantation. These findings suggest a regenerative approach for cartilage and synovial joint defects that can potentially be translated into patients with arthritis, trauma, or osteonecrosis. Cell homing, instead of cell delivery, might accelerate therapeutic translation.

Acknowledgments

This work was supported by a research grant from the New York State Stem Cell Science and US National Institutes of Health grant R01EB002332. We thank ICM staff at Columbia University Medical Center for veterinary assistance, and members of J J M laboratory for administrative and additional technical support. Synovium cells were a generous gift from Elena Jones of University of Leeds, UK.

References

1. Levenberg S, Rouwkema J, Macdonald M, et al. Engineering vascularized skeletal muscle tissue. Nat Biotechnol. 2005; 23:879–84. [PubMed: 15965465]
2. Zimmermann WH, Melnychenko I, Wasmeier G, et al. Engineered heart tissue grafts improve systolic and diastolic function in infarcted rat hearts. Nat Med. 2006; 12:452–58. [PubMed: 16582915]
3. Atala A, Bauer SB, Soker S, Yoo JJ, Retik AB. Tissue-engineered autologous bladders for patients needing cystoplasty. Lancet. 2006; 367:1241–46. [PubMed: 16631879]
4. Sacco A, Doyonnas R, Kraft P, Vitorovic S, Blau HM. Self-renewal and expansion of single transplanted muscle stem cells. Nature. 2008; 456:502–06. [PubMed: 18806774]
5. Yang R, Chen M, Lee CH, Yoon R, Lal S, Mao JJ. Clones of ectopic stem cells colonize muscle defects in vivo. PloS One. (in press).
6. Fodor WL. Tissue engineering and cell based therapies, from the bench to the clinic: the potential to replace, repair and regenerate. Reprod Biol Endocrinol. 2003; 1:102. [PubMed: 14614775]
7. Muschler GF, Raut VP, Patterson TE, Wenke JC, Hollinger JO. The design and use of animal models for translational research in bone tissue engineering and regenerative medicine. Tissue Eng Part B Rev. 2010; 16:123–45. [PubMed: 19891542]
8. Prockop DJ. Repair of tissues by adult stem/progenitor cells (MSCs): controversies, myths, and changing paradigms. Mol Ther. 2009; 17:939–46. [PubMed: 19337235]
9. Laird DJ, von Andrian UH, Wagers AJ. Stem cell trafficking in tissue development, growth, and disease. Cell. 2008; 132:612–30. [PubMed: 18295579]
10. Karp JM, Leng Teo GS. Mesenchymal stem cell homing: the devil is in the details. Cell Stem Cell. 2009; 4:206–16. [PubMed: 19265660]
11. Agrawal V, Johnson SA, Reing J, et al. Epimorphic regeneration approach to tissue replacement in adult mammals. Proc Natl Acad Sci USA. 2009; 107:3351–55. [PubMed: 19966310]
12. Si Y, Tsou CL, Croft K, Charo IF. CCR2 mediates hematopoietic stem and progenitor cell trafficking to sites of inflammation in mice. J Clin Invest. 2010; 120:1192–203. [PubMed: 20234092]
13. Park DK, Della Valle CJ, Quigley L, Moric M, Rosenberg AG, Galante JO. Revision of the acetabular component without cement. A concise follow-up, at 20 to 24 years, of a previous report. J Bone Joint Surg Am. 2009; 91:350–55. [PubMed: 19181979]
14. Lawrence RC, Helmick CG, Arnett FC, et al. Estimates of the prevalence of arthritis and selected musculoskeletal disorders in the United States. Arthritis Rheum. 1998; 41:778–99. [PubMed: 9588729]
15. Goldberg, VM.; Caplan, AI. Orthopedic tissue engineering: basic science and practices. New York, USA: Informa Health Care; 2004.

16. Gao J, Dennis JE, Solchaga LA, Goldberg VM, Caplan AI. Repair of osteochondral defect with tissue-engineered two-phase composite material of injectable calcium phosphate and hyaluronan sponge. Tissue Eng. 2002; 8:827–37. [PubMed: 12459061]
17. Jiang CC, Chiang H, Liao CJ, et al. Repair of porcine articular cartilage defect with a biphasic osteochondral composite. J Orthop Res. 2007; 25:1277–90. [PubMed: 17576624]
18. Scotti C, Tonnarelli B, Papadimitropoulos A, et al. Recapitulation of endochondral bone formation using human adult mesenchymal stem cells as a paradigm for developmental engineering. Proc Natl Acad Sci USA. 2010; 107:7251–56. [PubMed: 20406908]
19. Noh MJ, Copeland RO, Yi Y, et al. Pre-clinical studies of retrovirally transduced human chondrocytes expressing transforming growth factor-beta-1 (TG-C). Cytotherapy. 2010; 12:384–93. [PubMed: 20370350]
20. Hunziker EB. Growth-factor-induced healing of partial-thickness defects in adult articular cartilage. Osteoarthritis Cartilage. 2001; 9:22–32. [PubMed: 11178944]
21. Erggelet C, Endres M, Neumann K, et al. Formation of cartilage repair tissue in articular cartilage defects pretreated with microfracture and covered with cell-free polymer-based implants. J Orthop Res. 2009; 27:1353–60. [PubMed: 19382184]
22. Buckwalter JA, Martin JA. Osteoarthritis. Adv Drug Deliv Rev. 2006; 58:150–67. [PubMed: 16530881]
23. Mao JJ. Stem-cell-driven regeneration of synovial joints. Biol Cell. 2005; 97:289–301. [PubMed: 15836429]
24. Wood JJ, Malek MA, Frassica FJ, et al. Autologous cultured chondrocytes: adverse events reported to the United States Food and Drug Administration. J Bone Joint Surg Am. 2006; 88:503–07. [PubMed: 16510814]
25. Jain RK, Au P, Tam J, Duda DG, Fukumura D. Engineering vascularized tissue. Nat Biotechnol. 2005; 23:821–23. [PubMed: 16003365]
26. Lee CH, Marion NW, Hollister S, Mao JJ. Tissue formation and vascularization in anatomically shaped human joint condyle ectopically in vivo. Tissue Eng Part A. 2009; 15:3923–30. [PubMed: 19563263]
27. Marion NW, Mao JJ. Mesenchymal stem cells and tissue engineering. Methods Enzymol. 2006; 420:339–61. [PubMed: 17161705]
28. Boschetti F, Peretti GM. Tensile and compressive properties of healthy and osteoarthritic human articular cartilage. Biorheology. 2008; 45:337–44. [PubMed: 18836234]
29. Chu CR, Szczodry M, Bruno S. Animal models for cartilage regeneration and repair. Tissue Eng Part B Rev. 2010; 16:105–15. [PubMed: 19831641]
30. Alhadlaq A, Mao JJ. Tissue-engineered osteochondral constructs in the shape of an articular condyle. J Bone Joint Surg Am. 2005; 87:936–44. [PubMed: 15866954]
31. Almarza AJ, Athanasiou KA. Design characteristics for the tissue engineering of cartilaginous tissues. Ann Biomed Eng. 2004; 32:2–17. [PubMed: 14964717]
32. Moioli EK, Hong L, Guardado J, Clark PA, Mao JJ. Sustained release of TGFbeta3 from PLGA microspheres and its effect on early osteogenic differentiation of human mesenchymal stem cells. Tissue Eng. 2006; 12:537–46. [PubMed: 16579687]
33. Moioli EK, Hong L, Mao JJ. Inhibition of osteogenic differentiation of human mesenchymal stem cells. Wound Repair Regen. 2007; 15:413–21. [PubMed: 17537129]
34. Woodfield TB, Guggenheim M, von Rechenberg B, Riesle J, van Blitterswijk CA, Wedler V. Rapid prototyping of anatomically shaped, tissue-engineered implants for restoring congruent articulating surfaces in small joints. Cell Prolif. 2009; 42:485–97. [PubMed: 19486014]
35. Jones EA, Crawford A, English A, et al. Synovial fluid mesenchymal stem cells in health and early osteoarthritis: detection and functional evaluation at the single-cell level. Arthritis Rheum. 2008; 58:1731–40. [PubMed: 18512779]
36. Koga H, Muneta T, Ju YJ, et al. Synovial stem cells are regionally specified according to local microenvironments after implantation for cartilage regeneration. Stem Cells. 2007; 25:689–96. [PubMed: 17138960]

37. Djouad F, Bony C, Haupl T, et al. Transcriptional profiles discriminate bone marrow-derived and synovium-derived mesenchymal stem cells. Arthritis Res Ther. 2005; 7:R1304–15. [PubMed: 16277684]

38. Perrin, DE.; English, JP. Polycaprolactone. In: Domb, AJ.; Kost, J.; Wiseman, DM., editors. Handbook of biodegradable polymers. Chur, Switzerland: Harwood Academic Publishers; 1997. p. 63-77.

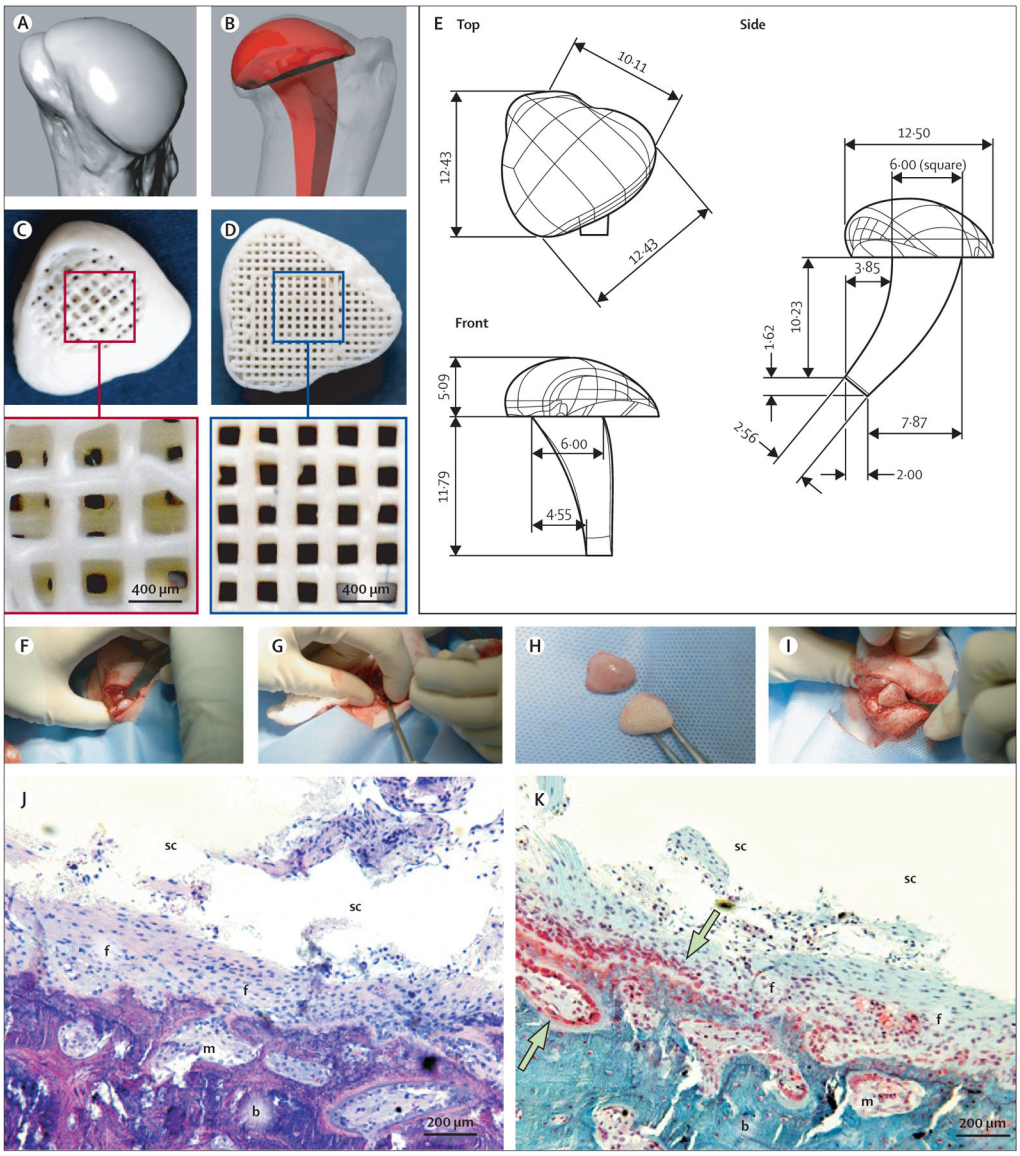

Figure 1. Surgical replacement of synovial joint

Surface morphology of a rabbit joint was reconstructed (A) to design an anatomically correct bioscaffold (B) with an intramedullary stem. A 200-μm thick shell was designed, along with internal microchannels opening to the synovium cavity (C) and bone marrow (D). PCL-HA was used to fabricate bioscaffolds following computer-aided design (E). The humeral head was excised at its metaphysis junction (F), and an orthopaedic drill used to create an intramedullary tunnel for stem fixation (G). The bioscaffold (H) was implanted by press-fitting (I). In defect-only rabbits, haematoxylin and eosin staining 4 months after surgery (J) showed that little bone had regenerated in the defect; the synovial joint cavity (sc) was visible with fibrous tissue (f) covering bone and marrow (m). Safranin O staining (K) showed scarce chondrocyte-like cells (shown by arrows) in the defect area in the synovial cavity. PCL-HA=poly-ε-caprolactone hydroxyapatite.

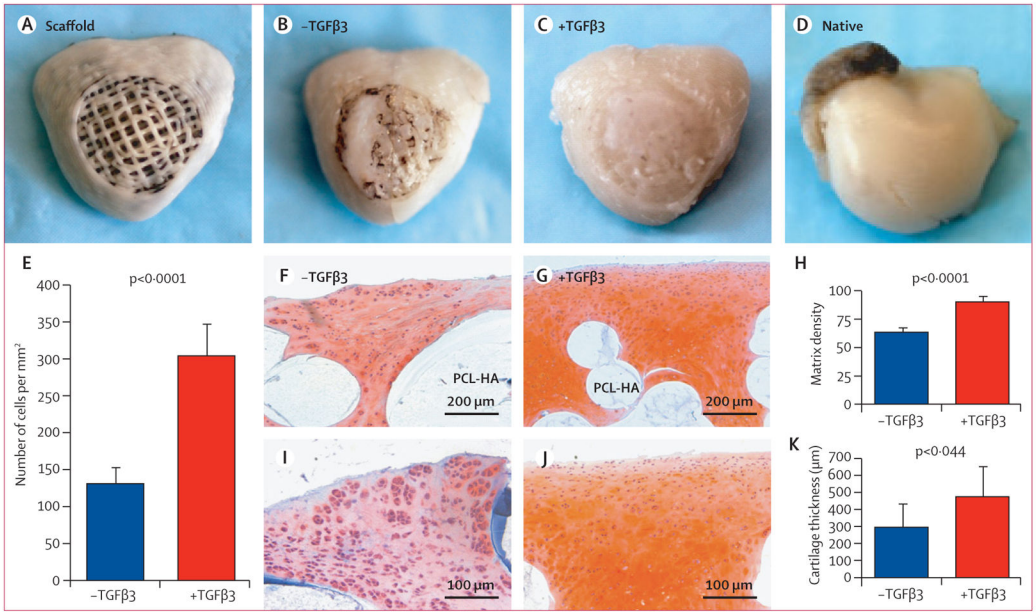

Figure 2. Articular cartilage regeneration

India ink staining of (A) unimplanted bioscaffold, (B) TGFβ3-free and (C) TGFβ3-infused bioscaffolds after 4 months' implantation, and (D) native cartilage. (E) Number of chondrocytes present in TGFβ3-infused and TGFβ3-free regenerated articular cartilage samples (n=8 per group). Safranin O staining of TGFβ3-free (F, I) and TGFβ3-infused (G, J) articular cartilage. Matrix density (H) and cartilage thickness (K) of TGFβ3-infused and TGFβ3-free samples (n=8 per group for both comparisons). TGFβ3=transforming growth factor β3. PCL-HA=poly-ε-caprolactone hydroxyapatite.

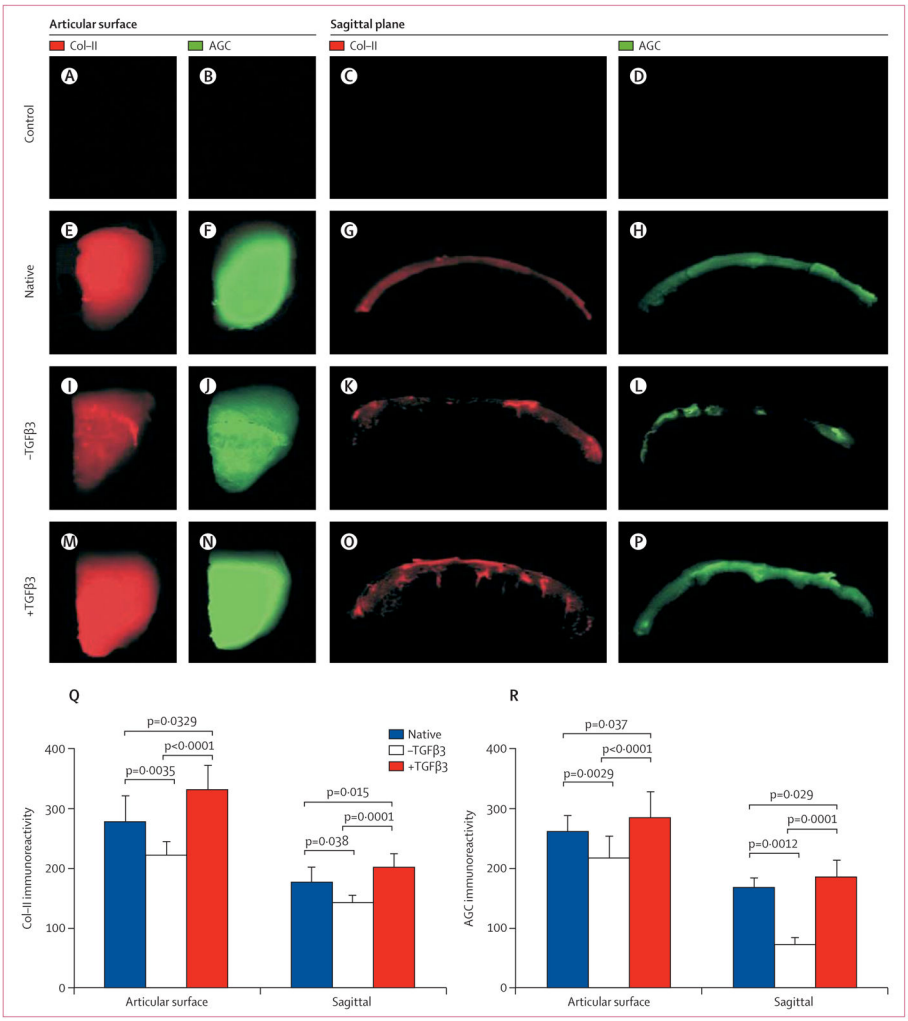

Figure 3. TGFβ3 delivery and quality of articular cartilage

Immunostaining for Col-II and AGC in unimplanted bioscaffold (A–D) and native (E–H), TGFβ3-free (I–L), and TGFβ3-infused (M–P) articular cartilage samples. Immunoreactivity for Col-II (Q) and AGC (R) in native, TGFβ3-free, and TGFβ3-infused samples (n=10 per group). Col-II=collagen type II. AGC=aggrecan. TGFβ3=transforming growth factor β3.

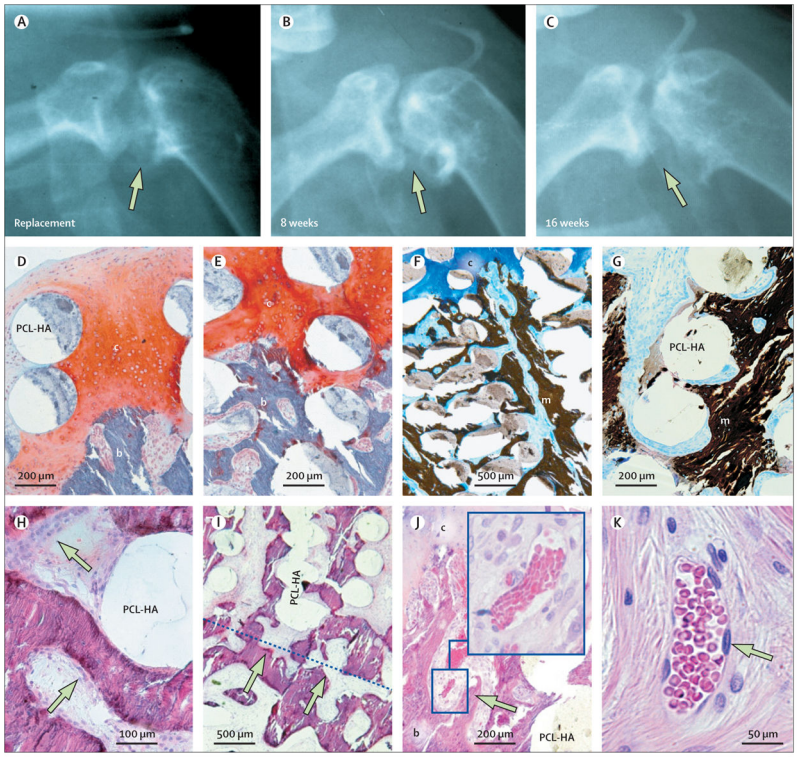

Figure 4. Vascularisation of regenerated subchondral bone

(A) Radiolucency (shown by arrow) was present in the joint cavity on excision of the condylar head. By 8 weeks (B) and 16 weeks (C) after surgery, a convex radio-opaque structure in the shape of articular condyle was present. (D) After 16 weeks' implantation, regenerated cartilage (c) extended to subchondral bone (b), which consisted of trabecular structures (E). (F, G) Von Kossa staining indicated mineral deposition that extended from the cartilage region (c, blue area) longitudinally in microchannels (m). (H) Bone trabeculae were populated by columnar osteoblast-like cells (which are shown by arrows). (I) Regenerated bone integrated to native humeral bone (arbitrary boundary shown by dashed blue line). (J) Multiple blood vessels (example shown by arrow) were present in regenerated bone. High magnification (K) showed the presence of erythrocytes within the lumen of an endothelium-lined blood vessel (arrow). PCL-HA=poly-ε-caprolactone hydroxyapatite.

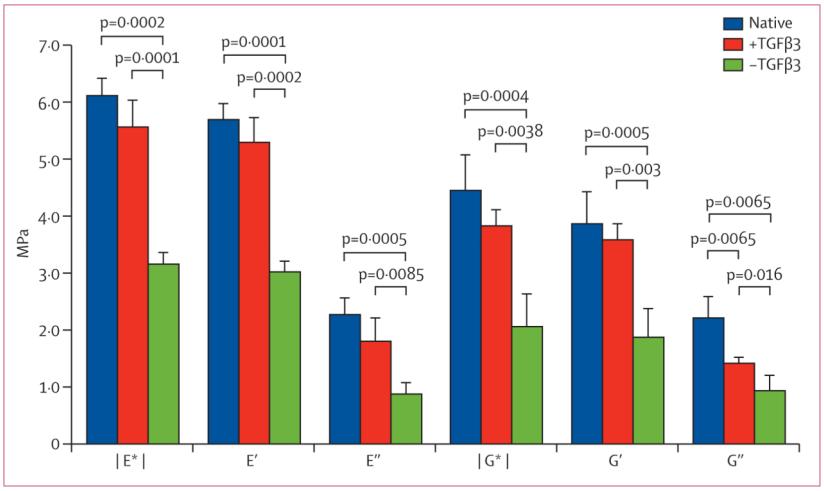

Figure 5. Mechanical properties of regenerated cartilage

E*=complex compressive modulus. E′=storage modulus. E″=loss modulus. G*=complex shear modulus. G′=shear storage modulus. G″=shear loss modulus. TGFβ3=transforming growth factor β3.